



Published in final edited form as:

Curr Biol. 2017 October 23; 27(20): 3168–3177.e3. doi:10.1016/j.cub.2017.08.068.

Early pheromone experience modifies a synaptic activity to influence adult pheromone-responses of *C. elegans*

Myeongjin Hong^{1,8}, Leesun Ryu^{1,8}, Maria C. Ow², Jinmahn Kim¹, A Reum Je³, Satya Chinta⁴, Yang Hoon Huh³, Kea Joo Lee⁵, Rebecca A. Butcher⁴, Hongsoo Choi⁶, Piali Sengupta⁷, Sarah E. Hall², and Kyuhyung Kim^{1,9,*}

¹Department of Brain and Cognitive Sciences, DGIST, Daegu, 42988, Republic of Korea

²Department of Biology, Syracuse University, Syracuse, NY 13044, USA

³Center for Electron Microscopy Research, Korea Basic Science Institute, Cheongju-si, Chungcheongbuk-do, 28119, Republic of Korea

⁴Department of Chemistry, University of Florida, Gainesville, FL32611, USA

⁵Korea Brain Research Institute, Daegu, 41068, Republic of Korea

⁶Robotics Engineering Department, DGIST, Daegu, 42988, Republic of Korea

⁷Department of Biology and National Center for Behavioral Genomics, Brandeis University, Waltham, MA02454, USA

SUMMARY

Experiences during early development can influence neuronal functions and modulate adult behaviors [1, 2]. However, the molecular mechanisms underlying the long-term behavioral effects of these early experiences are not fully understood. The *C. elegans* *ascr#3* (*asc-0394C9*, *C9*) pheromone triggers avoidance behavior in adult hermaphrodites [3–7]. Here, we show that hermaphrodites that are briefly exposed to *ascr#3* immediately after birth exhibit increased *ascr#3*-specific avoidance as adults indicating that *ascr#3*-experienced animals form a long lasting memory or imprint of this early *ascr#3* exposure [8]. *Ascr#3* imprinting is mediated by increased synaptic activity between the *ascr#3*-sensing ADL neurons and their post-synaptic SMB motor neuron partners via increased expression of the *odr-2* GPI-linked signaling gene in the SMB neurons. Our study suggests that the memory for early *ascr#3* experience is imprinted via alteration of activity of a single synaptic connection, that in turn shapes experience-dependent plasticity in adult *ascr#3* responses.

*Correspondence: khkim@dgist.ac.kr.

⁸Co-first author

⁹Lead Contact

Publisher's Disclaimer: This is a PDF file of an unedited manuscript that has been accepted for publication. As a service to our customers we are providing this early version of the manuscript. The manuscript will undergo copyediting, typesetting, and review of the resulting proof before it is published in its final citable form. Please note that during the production process errors may be discovered which could affect the content, and all legal disclaimers that apply to the journal pertain.

Author contributions

M.H., L.S., M.O., and A.R.J. performed the experiments; J.K., S.C., R.A.B. and H.C. provides reagents; M.H., L.S., M.O., Y.H.H., K.J.L. P.S., S.E.H. and K.K. analyzed and interpreted data; M.H., L.S., P.S., S.E.H., and K.K wrote the manuscript.

Keywords

sensory imprinting; pheromone; synapse; neuronal activity; GPI-anchored protein

RESULTS

Adult *C. elegans* transiently exposed to *ascr#3* during larval stages exhibits increased *ascr#3* pheromone avoidance

To assess whether early experience of pheromones affects *ascr#3* avoidance behavior in adult worms, we transiently exposed first larval stage (L1) wild-type worms to *ascr#3* and examined their responses to *ascr#3* as adults (Figure 1A and see STAR methods). To test avoidance, a pheromone diluted in buffer was applied to a freely moving animal and the fraction of animals that reverse was calculated (drop test assay; See STAR Methods) [9]. Pre-exposure to 600 nM *ascr#3* during the L1 stage significantly improved adult avoidance of *ascr#3* at concentrations that elicit only weak avoidance by adults that were not similarly pre-exposed, but did not further increase avoidance at higher *ascr#3* concentrations (Figure 1B). Increased *ascr#3* avoidance appeared to be mediated by increased long reversals and omega turns but not short reversals in pre-exposed animals (Figure S1A). Henceforth, we calculate increased avoidance as a learning index (LI: pre-exposed reversing rate minus naive reversing rate/100) (Figure 1C).

We next defined the optimal *ascr#3* concentration that elicits the pre-exposure effect. Animals exhibited maximal adult *ascr#3* avoidance when they were pre-exposed to *ascr#3* concentrations higher than 600 nM (Figure 1D) [4]. Although exposure of L1 larvae to *ascr#3* pheromone also promotes entry into the alternate dauer developmental stage, we note that the conditions used for imprinting are distinct from those used for dauer induction, and few if any *ascr#3*-imprinted animals enter into the dauer stage. These results indicate that early experience of *ascr#3* pheromone appears to be translated into behavioral changes in the adult stage of hermaphrodites, suggesting that *ascr#3*-experienced animals form a long-lasting memory or imprint for *ascr#3*. Wild-type *C. elegans* males exhibit neutral responses to 100 nM *ascr#3* [7, 10]. We found that *ascr#3*-experienced adult males continue to exhibit neutral responses to 100 nM *ascr#3* (Figure S1B), indicating that early *ascr#3* experience appears to increase *ascr#3* avoidance only by adult hermaphrodites but not by adult males.

The memory for *ascr#3* is acquired during the L1 larval stage

To determine whether the long-lasting memory for *ascr#3* is formed during a specific developmental time window, worms were pre-exposed to *ascr#3* at multiple developmental stages and their *ascr#3* responses were assessed as adults. All assays were conducted by pre-exposing animals to 600 nM pheromone and assessing responses to 100 nM pheromone, unless noted otherwise.

Compared to the L1 stage, *ascr#3* pre-exposure at the L3, L4, or adult stages did not enhance *ascr#3* avoidance in adults (Figure 1E), suggesting that the L1 stage is critical for acquiring the *ascr#3* memory. We could not test the L2 stage because of complexity with dauer formation [11]. We further defined the time window within the L1 stage necessary for this

behavior, and found that pre-exposure in a defined time period during the early L1 stage (up to 6 hours following hatching at 20 °C) appears to represent the critical period for formation of the *ascr#3* memory (Figure 1E). More specifically, exposure of *ascr#3* to worms at 2–6 hour after birth appears to be necessary and sufficient for the increased *ascr#3* avoidance (Figure 1F).

C. elegans secretes additional pheromones, including *ascr#2*, *ascr#5*, and *icas#9*. Similar to *ascr#3*, these pheromones are also potent inducers of entry into the alternate dauer developmental stage under limiting food conditions [4]. Pre-exposure to 600 nM *ascr#2* or *ascr#5* alone did not affect *ascr#3* avoidance by adults, suggesting that pheromone imprinting does not reflect a memory of general unfavorable dauer inducing conditions but specifically encodes experience of the *ascr#3* pheromone (Figure 1G). Pre-exposure to mixtures of *ascr#2*, *ascr#5*, and *icas#9* with *ascr#3* also did not affect *ascr#3* imprinting, further supporting that imprinting is specific to *ascr#3* (Figure 1H). Moreover, pre-exposure to *ascr#2* did not result in altered adult avoidance of *ascr#2* (Figure S1C), further confirming specificity of this process to *ascr#3*. In addition, pre-exposure to *ascr#3* did not affect high-osmolality glycerol avoidance (Figure S1D), suggesting that early *ascr#3* experience does not affect broad avoidance behaviors to other repulsive chemicals by adults. However, we are unable to exclude the possibility that imprinting by other ascarosides may occur at developmental stages other than the L1 stage.

Since the memory for a specific pheromone component is acquired only at the critical developmental period, we further define this altered *ascr#3* avoidance as sensory imprinting [8]. Interestingly, when animals recovered from the developmentally arrested dauer stage that was induced by limited food supply in the presence of pheromones including *ascr#3* at the L1 and L2 stages, their *ascr#3* avoidance was comparable to or even weaker than that of naive animals (Figure S1E) [11]. These data indicate that the *ascr#3* imprint appears to be removed following dauer experience and/or *ascr#3* imprinting requires non dauer-inducing conditions at the L1 stage. Moreover, it is likely that passage through the dauer stage results in genome-wide changes in gene expression patterns [12, 13], which may mask or erase *ascr#3* imprinting phenotypes.

We next investigated perdurance of the *ascr#3* memory. We found that pre-exposed 3 or 6 day-old adults still exhibited increased *ascr#3* avoidance (Figure S1F). We also asked whether memories are transmitted to the next generation but found that progeny from imprinted mothers did not exhibit improved *ascr#3* avoidance (Figure S1G). These results indicate that the *ascr#3* imprint lasts with aging but is not inherited under these assay conditions.

***odr-2* acts in the SMB neurons to increase *ascr#3* avoidance in *ascr#3* imprinted animals**

We next performed a candidate gene search to identify genes and molecules required for *ascr#3* imprinting. We first tested genes that have been shown to be required for distinct forms of learning and memory in *C. elegans*. These include the *egl-4* (cyclic GMP-dependent protein kinase) gene implicated in sensory adaptation, the *casy-1* (calsyntenin) gene involved in associative learning, and the *sra-11* (7-TM G protein-coupled receptor), *ttx-3* (LIM homeodomain protein), or *tdc-1* (tyrosine decarboxylase) genes involved in

olfactory imprinting [14–17]. However, loss of function of these genes did not affect *ascr#3* imprinting (Figure S2A).

In the course of analyzing mutants defective in odorant responses, we found that *odr-2* (*n2145*) [18, 19] mutants exhibited defects in *ascr#3* imprinting although the ability of these mutants to avoid *ascr#3* was unaffected (Figure 2A, 2B). The *ascr#3* imprinting defects in *odr-2* mutants were fully rescued upon expression of wild-type *odr-2* cDNA driven under its upstream regulatory sequences (Figure 2C). The *odr-2* gene encodes a membrane-associated protein related to the Ly-6 (leukocyte antigen-6) superfamily of GPI (glycosylated phosphatidylinositol)-linked proteins, and *odr-2* mutants have previously been shown to exhibit decreased chemotaxis towards a set of volatile attractive chemicals [19]. *odr-2* is expressed in a set of head neurons including RIG, RME and SMB [19, 20]. To determine where ODR-2 acts to regulate *ascr#3* imprinting, we tested transgenic animals expressing *odr-2* wild-type sequences for rescue of the *ascr#3* imprinting defects. We found that while expression of *odr-2* in RIG and RME under the control of *odr-2* (–377) promoter [20] did not rescue these behavioral defects, *ascr#3* imprinting defects were fully restored upon expression of *odr-2* exclusively in SMB under the control of *flp-12* (–339) promoter (Figure 2D) [20], indicating that ODR-2 acts in the SMB neurons to mediate *ascr#3* imprinting.

The SMB neurons consist of two left and right pairs (dorsal or ventral) of sensory/inter/motor neuron types that are located in the head, and that innervate the head and neck muscles (Figure 2E) [21]. While their synapse-free processes extend along the ventral or dorsal sublateral cords to the tail, the SMB neurons have extensive electric and chemical synaptic contacts to other neurons in the head [21]. These neurons regulate head locomotion [20–22]. However, their roles in chemosensory behaviors have not been explored. We next investigated that the SMB neurons are required for *ascr#3* imprinting. To address this issue, we examined *lim-4* mutants in which the SMB neurons are not fully differentiated and in which the functions of SMB are completely abolished [20]. *lim-4* mutants had been shown to exhibit additional defects including neuronal specification [23]. While *lim-4* mutants were still able to avoid *ascr#3*, pre-exposure to *ascr#3* did not enhance *ascr#3* avoidance in *lim-4* mutants (Figure 2F). These results together with *odr-2* rescue results support that the SMB neurons may play an important role in *ascr#3* imprinting.

Ascr#3-induced responses in the ADL chemosensory neurons are unaltered in *ascr#3* imprinted worms

In adults, *ascr#3* elicits avoidance behavior in hermaphrodites via the nociceptive ADL chemosensory neurons (Figure 3A) [7]. To describe the neuronal basis of pheromone imprinting, we first monitored intracellular Ca^{2+} dynamics in response to *ascr#3* in transgenic animals expressing the genetically encoded calcium sensor GCaMP3 in the *ascr#3*-sensing ADL neurons. The ADL neurons exhibit a rapid and transient Ca^{2+} increase upon exposure to nano-molar concentrations of *ascr#3* (Figure 3B) [7]. Both naive animals and *ascr#3*-imprinted animals displayed similar Ca^{2+} transients in adult ADL neurons upon addition of *ascr#3* (Figure 3B). These results suggest that increased *ascr#3* avoidance is not due to enhanced sensory responsiveness of ADL. Furthermore, consistent with the normal

ascr#3 avoidance behavior of *odr-2* mutants, the ADL Ca²⁺ response to ascr#3 was not altered in *odr-2* mutants (Figure 3C).

The ADL sensory neurons drive ascr#3 avoidance through their chemical synapses [7]. Inspection of the anatomical wiring data from the *C. elegans* connectome suggests that ascr#3 signals from the ADL neurons are transmitted to a few major postsynaptic target neurons including AIB (1st layer interneurons), and the AVA and AVD backward command interneurons (Figure 3A). Previous studies have shown that activity in AIB, AVA and AVD is increased during backward movement or reversals [24]. We found that while the AIB or AVD neurons exhibited noisy but low levels of Ca²⁺ responses upon exposure to ascr#3 (Figure S3A, S3B), the AVA cell bodies responded strongly and consistently to repeated ascr#3 addition with increased Ca²⁺ levels (Figure 3D). However, these responses were unaltered upon ascr#3 imprinting (Figure 3D, Figure S3A, S3B). These results imply that ascr#3 signals in the ADL neurons may be transmitted mainly via AVA, but that imprinting does not enhance ascr#3 avoidance via this ADL-AVA circuit.

The SMB neurons mediate increased ascr#3 avoidance in ascr#3 imprinted animals

The *C. elegans* connectome data indicate that the SMBV neurons are additional postsynaptic partners of the ADL sensory neurons (Figure 3A) although the synaptic strength appears to be weak. Since the SMB neurons appear to play a role in ascr#3 imprinting, we then examined how SMB is involved in ascr#3 avoidance behavior.

We first expressed GCaMP3 in SMB under the control of *flp-12(-339)* promoter that drives transgene expression in all four SMB neurons [20]. We note that a SMBV-specific promoter is not currently available. Moreover, since the cell bodies of SMBD and SMBV are located in close proximity, differentiating among these neurons is challenging [20]. We thus examined ascr#3 responses in all SMB neurons together. Acute ascr#3 exposure did not elicit Ca²⁺ transients in the SMB neurons of naive control animals (Figure 4A, Movie S1). However, we detected consistent and robust Ca²⁺ transients in response to acute ascr#3 exposure in ascr#3 imprinted animals (Figure 4A, Movie S2). Since SMB may detect body muscle contractions that could be responsible for the observed Ca²⁺ responses in SMB, we paralyzed worms with the nicotinic acetylcholine receptor agonist levamisole. Levamisole-treated ascr#3 imprinted animals still exhibited similar or even enhanced Ca²⁺ dynamics upon ascr#3 exposure (Figure S4A).

To test whether the observed Ca²⁺ transients in SMB in ascr#3 imprinted animals are transmitted from ADL, we examined Ca²⁺ responses in transgenic animals expressing TeTx (tetanus toxin light chain) specifically in the ADL neurons to block synaptic transmission from ADL [7]. Ca²⁺ transients of SMB in ascr#3 imprinted animals were strongly suppressed by blocking ADL synaptic transmission (Figure 4B, Figure S4B), suggesting that ascr#3 imprinting results in enhanced ascr#3 signal transmission from ADL to SMB. These results indicate that ascr#3 imprinting specifically alters the ADL-SMB synaptic transmission.

Moreover, the ascr#3 imprinting-dependent Ca²⁺ response in SMB was completely abolished in *odr-2* mutants (Figure 4C), indicating that *odr-2* elicits increased activity of

SMB to *ascr#3* exposure in imprinted animals by enhancing the ADL-SMB synaptic transmission.

Upregulation of *odr-2* expression of L1 larvae is sufficient for increased *ascr#3* avoidance in adults

To further investigate the role of *odr-2* in mediating increased SMB activity in of *ascr#3* imprinted animals, we monitored *odr-2* expression in SMB and found that *odr-2* expression in SMB was increased after transient exposure to *ascr#3* at the L1 stage and was maintained through adulthood (Figure 4D). In contrast, *odr-2p::gfp* expression was unaffected in other *odr-2*-expressing cells including RIG and RME (Figure 4D). To examine whether upregulation of *odr-2* at the L1 stage is sufficient for the increased *ascr#3* avoidance in adults, we expressed *odr-2* cDNA in wild-type animals with the inducible expressed heat-shock promoter. Compared to animals with no heat-shock treated or those heat-shocked only at the adult stage, transient induction of *odr-2* gene activity at the L1 larval stage was sufficient to increase *ascr#3* avoidance in adults (Figure 4E). Thus far, our results are consistent with a model in which the increased *odr-2* expression in SMB of the *ascr#3* imprinted animals causes functional changes in the ADL-SMB synaptic activities.

DISCUSSION

The well-defined nervous system of *C. elegans* with only 302 neurons mediates a broad spectrum of behaviors. However, these behaviors are plastic and can be modulated by the animal's experience [25, 26]. For example, *C. elegans* is able to constantly monitor and adapt to their environment by forming short-term and/or long-term memories in their hard-wired neural circuits (See a review by [27]). *C. elegans* has also been shown to imprint long-term memories of environments, including odor or pathogen exposure experienced during development, via largely uncharacterized mechanisms [15, 17]. Here, we show a novel imprinting paradigm in *C. elegans* where exposure of newly hatched animals to the *ascr#3* pheromone increases adult neuronal activity in response to *ascr#3*, resulting in altered behavior. Since the long-lasting memory for *ascr#3* pheromone is formed during a critical period of early development and shapes the *ascr#3* avoidance behavior of adults, this learning and long-term memory process for the pheromone could be referred to as sensory imprinting [8]. Sensory imprinting is a form of long-term memory that occurs in many animals: for example, homing of salmon and neonatal attachment of rodents [28, 29]. This type of behavioral plasticity could be essential for animal survival in natural environments. *Ascr#3* is the most abundant and potent aversive pheromone in *C. elegans* hermaphrodites and may represent conditions of overcrowding [7, 30, 31]. Thus, newly hatched worms may pair this specific *ascr#3* pheromone memory to their neuronal activity to promote searching behavior for more favorable environments as adults or to shape currently unidentified behavioral or physiological states for optimal fitness.

We previously showed that the ADL sensory neurons detect *C. elegans* pheromone *ascr#3* and drive *ascr#3* avoidance through their chemical synapses [7]. The ADL neurons directly connect to more than twenty postsynaptic neurons, and inspection of the anatomical wiring data including the number of synapses led us to hypothesize that *ascr#3* signals from ADL

are transmitted to the three major post-synaptic target neurons including the AIB, AVA and AVD interneurons. In this work, we have found that under non-*ascr#3* pre-exposed (naive) conditions the *ascr#3* signals are transmitted via the ADL-AVA synapses (Figure 4F). However, while transient exposure to *ascr#3* at the L1 larval stage does not appear to affect this ADL-AVA synaptic transmission, this experience instead increases the ADL-SMB synaptic activities which are normally inactive in naive animals, and may account for the observed enhanced *ascr#3* avoidance behavior in adult worms (Figure 4F).

The conclusion that the SMB neurons are the critical site for mediating *ascr#3* imprinting is supported by these findings: 1) The SMB neurons respond to *ascr#3* exposure in *ascr#3*-imprinted but not in naive animals; 2) Expression of *odr-2* that is necessary and partly sufficient for *ascr#3* imprinting is increased specifically in SMB of *ascr#3*-imprinted animals; 3) *lim-4* mutants in which SMB functions are abolished fail to imprint *ascr#3* experience. Laser ablation of the SMB motor neurons causes increased reversal frequency and wave amplitude of forward locomotion [20, 22]. Since the SMB neurons innervate head and neck muscles, and *ascr#3* exposure now activates the SMB neurons in *ascr#3* imprinted animals, our results suggest that early *ascr#3* experience causes the SMB neurons to sensitize to subsequent *ascr#3* exposure and modulate backward movement via the alteration of head/neck muscle activity (Figure 4F). For example, in addition to body muscle contraction triggered by ADL-AVA synaptic transmission, head/neck muscle contraction due to enhanced SMB neuronal activities upon *ascr#3* imprinting may increase reversal rates further [24, 32] or the SMB neurons could directly activate backward motor circuits via interneurons including the SAA neurons [21].

Our data show that *odr-2* is essential for *ascr#3* imprinting. *odr-2* encodes a novel protein distantly related to murine Ly6 lymphocyte antigen protein that is tethered to membrane by a GPI (glycosylphosphatidylinositol) anchor [19]. In vertebrates, GPI anchored proteins have roles in development and neurogenesis by regulating several signaling pathways including Notch, Wnt or TGF β [33]. Moreover, a set of Ly6 related genes including *Lynx1* and *Lynx2* have been shown to be expressed in the nervous system and appear to be accessory components of nicotinic acetylcholine receptors, thus modulating their functions [34, 35]. Our results indicate that the ODR-2 GPI anchored protein changes synaptic activity between ADL and SMB. ODR-2 proteins are localized on cell bodies and neuronal processes [36]. Thus, it is possible that ODR-2 may be co-localized with and regulate functions of neurotransmitter receptors in SMB.

Understanding how individual synapses are functionally or anatomically altered upon sensory imprinting is the essential first steps towards being able to dissect molecular and neuronal mechanisms underlying sensory imprinting and other forms of behavioral plasticity. Given that structures and functions of neural circuits are evolutionarily conserved, we expect that our work will lead to a general framework for understanding how circuits are modulated in higher animals including humans.

STAR METHODS

KEY RESOURCES TABLE

REAGENT or RESOURCE	SOURCE	IDENTIFIER
Chemicals, Peptides, and Recombinant Proteins		
Levamisole	Sigma	Cat# 16595-80-5
ascr #3	This paper	
Critical Commercial Assays		
PDMS Sylgard 184 Silicone Elastomer Kit	Dow Corning	Product code: 1064291
Experimental Models: Organisms/Strains : <i>C. elegans</i> strains		
<i>odr-2(n2145)</i> V	<i>Caenorhabditis</i> Genetics Center	RRID:WB-STRAIN:CX2304
<i>odr-2(n2145)</i> V; <i>IskEx606[odr-2 3p::odr-2cDNA]</i>	This paper	N/A
<i>odr-2(n2145)</i> V; <i>IskEx607[flp-12 3p::odr-2cDNA]</i>	This paper	N/A
<i>odr-2(n2145)</i> V ; <i>IskEx608[lim-4p::odr-2cDNA]</i>	This paper	N/A
<i>lim-4(ky403)</i> X	<i>Caenorhabditis</i> Genetics Center	RRID:WB-STRAIN:CX3937
<i>IskEx218[sre-1p::GCAMP3; unc-122p::dsRed]</i>	This paper	N/A
<i>odr-2(n2145)</i> V; <i>IskEx218[sre-1p::GCAMP3; unc-122p::dsRed]</i>	This paper	N/A
<i>IskEx597[nmr-1p::GCAMP3; unc-122p::dsRed]</i>	This paper	N/A
<i>IskEx113[flp-12 3p::GCAMP3; unc-122p::dsRed]</i>	This paper	N/A
<i>IskEx611[sre-1p::TeTx; unc-122p::gfp]; IskEx113[flp12 3p::GCAMP3]</i>	This paper	N/A
<i>odr-2(n2145)</i> V; <i>IskEx113[flp-12 3p::GCAMP3]</i>	This paper	N/A
<i>Isk Is11[odr-2p::gfp; unc-122p::dsRed]</i>	This paper	N/A
<i>IskEx418[hsp::odr-2cDNA; unc-122p::gfp]</i>	This paper	N/A
<i>IskEx895[avr-14p::gfp; unc-122p::dsRed]; IskEx28[flp-12p::mcherry; unc-122p::gfp]</i>	This paper	N/A
<i>odr-2(n2145); IskEx895[avr-14p::gfp; unc-122p::dsRed]; IskEx28[flp-12p::mcherry; unc-122p::gfp]</i>	This paper	N/A
<i>egl-4(ks60)</i> IV	<i>Caenorhabditis</i> Genetics Center	RRID:WB-STRAIN:FK223
<i>sra-11(ok630)</i> II	<i>Caenorhabditis</i> Genetics Center	RRID:WB-STRAIN:RB816
<i>odr-3(n2150)</i> V	<i>Caenorhabditis</i> Genetics Center	RRID:WB-STRAIN:CX2205
<i>odr-7(ky4)</i> X	<i>Caenorhabditis</i> Genetics Center	RRID:WB-STRAIN:CX4
<i>odr-10(ky32)</i> X	<i>Caenorhabditis</i> Genetics Center	RRID:WB-STRAIN:CX32
<i>casy-1(tm718)</i> II	National BioResource Project	N/A
<i>casy-1(pe401)</i> II	<i>Caenorhabditis</i> Genetics Center	RRID:WB-STRAIN:JN414
<i>ttx-3(ks5)</i> X	<i>Caenorhabditis</i> Genetics Center	RRID:WB-STRAIN:FK134
<i>tdc-1(n3419)</i> II	<i>Caenorhabditis</i> Genetics Center	RRID:WB-STRAIN:MT13113
<i>IskEx610[npr-9p::GCAMP3; unc-122p::dsRed]</i>	This paper	N/A
Software and Algorithms		
AxioVision software	Zeiss	RRID:SCR_002677
ZEN 2010 Lite Edition software	Zeiss	RRID:SCR_013672
ImageJ	https://imagej.nih.gov/ij/	RRID:SCR_003070
MATLAB	MathWorks	RRID:SCR_001622

REAGENT or RESOURCE	SOURCE	IDENTIFIER
Prism 5.0	GraphPad Software	RRID:SCR_002798
Adobe Illustrator CS6	Adobe	RRID:SCR_014198

Contact for Reagent and Resource Sharing

Further information and requests for resources and reagents should be directed to and will be fulfilled by the Lead Contact, Dr. Kyuhung Kim (khkim@dgist.ac.kr).

Experimental Model and Subject Details

C. elegans N2 strain was used as wild-type. Wild-type and transgenic animals were maintained at 20°C with abundant *E. coli* OP50 as food following standard conditions [37]. Day 1 (~24 hours after mid-L4 larval stage) young adult, hermaphrodite animals were used for experimentation, with the exception of the *odr-2p::gfp* quantification study in which the L1 stage animals were also assayed (Figure 4D).

Method Details

Generation of *C. elegans* transgenic lines—*odr-2 18a* cDNA was amplified with a set of primers containing restriction sites, 5'-*Age*I and 3'-*Not*I using PCR and inserted into pMC10 for performing the *odr-2* rescue experiment [19]. Upstream regulatory sequences, including *odr-2* (RIG, RME and SMB), *odr-2* (-377) (RIG and RME), *flp-12* (-339) (SMB), and *lim-4* (AWB, SAA, RID, RIV, RMD and SMB), were fused with *odr-2* cDNA to drive its expression in specific neurons [20]. To generate the *hsp::odr-2* cDNA transgene, the *hsp16.2* promoter was amplified from the *hsp16.2p::unc-3* cDNA transgene [38].

For Ca²⁺ imaging experiments of the AIB, AVD and AVA neurons, the promoter region of *sre-1p::GCaMP3* transgene was exchanged with *npr-9* (AIB) or *nmr-1* (AVD and AVA) promoters [7, 39]. *nmr-1p* was amplified from pCZGY1553 (a kind gift from Yishi Jin), and *npr-9p* was 2076 bp of upstream regulatory sequence amplified from genomic DNA by PCR. These promoters were ligated with GCaMP3 using the restriction sites, *Hind*III and *Bam*HI.

Each transgenic *C. elegans* strain was generated by microinjection of the rescue construct (10 ng/μl) with *unc-122p::dsRed* (50 ng/μl). The *hsp::odr-2* cDNA construct was injected with the *unc-122p::gfp* marker (50 ng/μl).

Pheromone imprinting—For pheromone imprinting, two types of 35 mm noble agar plates seeded with *E. coli* OP50 were made: the negative control plate contained distilled water (naive) and the experimental plate contained pheromones (pre-exposed). Figures 1G and 1H utilized experimental plates containing 600 nM *ascr#3*, *ascr#2* and *ascr#5*, and 600 nM *ascr#3*, *ascr#2*, *ascr#5* and *icas#9*, respectively. All other assays in this study used experimental plates containing 600 nM *ascr#3* for imprinting. To pre-expose animals to *ascr#3*, five 1-day-old young adult hermaphrodites were placed onto each control and experimental plate for 2~3 hours until 30 to 50 eggs were laid. After 1 day (~26 hr), the naive or pre-exposed L1 stage animals were transferred onto 60 mm nematode growth media plates seeded with *E. coli* OP50 food and grown for 2.5 days until the young adult stage. For

male imprinting experiments, we added ~20 males with L4 hermaphrodites for 1 day to mate and picked 5 adult hermaphrodites onto each naive and pre-exposed plates. For imprinting analysis of the next generation, 5 adults from naive or pre-exposed group (P0) were placed onto new control plates and allowed to lay 30~50 eggs (F1). The adults were then subsequently removed and the plates were incubated for 2.5 days at 20°C.

Post-dauer assay—Dauer formation assay was based on the protocol in [40]. 20 µl heat-killed OP50 was seeded onto 3.5 mm 600 nM *ascr#3* noble agar plates. 5~10 young adults were placed and discarded when over 50 eggs were obtained. The eggs were grown at 25°C for 68~72hr. Animals in dauer formation were picked onto new OP50 seeded 60 mm plates and grown at 20°C for 2~3 days. We assayed *ascr#3* avoidance with adult animals which were grown at 20°C as control.

Behavioral assay—The drop assay was performed as described with modifications [7]. All behavioral assays were performed in the absence of food and used 100 nM *ascr#3* diluted in M13 buffer (30 mM Tris-HCl [pH 7.0], 100 mM NaCl, 10 mM KCl), except Figure S1D which 200 mM glycerol was used [41]. To measure the percent of animals reversing upon *ascr#3* exposure, a young adult was transferred onto a plate without food and M13 buffer was dropped near the head of worm. If the worm failed to reverse in response to M13 after 10 seconds, *ascr#3* was dropped onto the front of the head and avoidance behaviors (reversal) were monitored for 10 seconds. Short or long reversals were defined as reversals with fewer than two head bends or more than two head bends, respectively [42]. Long reversals were counted as repulsion in this study. The imprinting index was calculated as the percentage of reversals of pre-exposed animals minus percentage of reversals of naive animals. Each assay tested the avoidance response of 10 young adult hermaphrodite animals, and at least 3 independent trials were performed.

In vivo calcium imaging—Calcium imaging experiments were performed as described previously [7], using microfluidics chips that were produced in-house with a custom made chrome mask and master mold [43]. Briefly, PDMS Sylgard 184 Silicone Elastomer Kit (Dow Corning) was solidified on the master mold at 70°C for 2 hours, and then was attached on a 24 × 24 mm glass coverslip using CUTE plasma equipment (Air) (FEMTOSCIENCE). The *C. elegans* transgenic strains used for calcium imaging experiments included *sre-1p::GCaMP3* (ADL), *flp-12(-339)p::GCaMP3* (SMB), *npr-9p::GCaMP3* (AIB) and *nmr-1p::GCaMP3* (AVA and AVD) were used [7]. Each animal was exposed to fluorescent light for 1~2 minutes and the images were captured under fixed exposure time (100ms) for 1 min with Zeiss Axioplan microscope using a 40X objective and a Zeiss AxioCam HR. The images were analyzed by AxioVision software, Image J, and custom-written scripts in MATLAB [7].

Levamisole treatment—25 mM levamisole (Sigma) was used to paralyze animals. 25 mM levamisole was diluted in M9 buffer from 0.25 M levamisole. The animals were placed into the solution for about 1 minute, during which pharyngeal pumping ceased, indicating paralysis.

Heat shock treatment—Heat shock treatment was performed as previously described [44]. After 16 hours from egg laying, animals were twice exposed to a 33°C heat shock for 30 minutes with a 1 hour recovery at 20°C in between. After the second heat shock treatment, the worms were incubated at 20°C until the adult stage and behavioral assays were performed (see above).

Quantification and Statistical analysis

Representative images—Images in Figures 4D and 4G were acquired using a Zeiss LSM700 Confocal microscope and Zeiss LSM780 Confocal microscope, respectively. The images were taken and analyzed through ZEN 2010 and Image J.

GFP quantification—For GFP quantification, the animals were anaesthetized by using 1 M NaN₃ and placed on 2 % agarose pad with a 24 × 24 mm cover slip. *odr-2p::gfp* strain was integrated using UV crosslinker (UVP). A minimum of 30 *odr-2p::gfp* animals were exposed to 100 mM ascr#3 or control plates at the L1 larval stage following the imprinting protocol described above and quantified for GFP fluorescence. GFP expression was scored under 40X objective Zeiss Axioplan microscopy by observing the brightness of the neuron cell body and process. The animals were observed under 40X objective Zeiss Axioplan microscopy and LSM700 Confocal microscope. The images were taken and acquired by AxioVision or Zen 2010. All strains were assayed in parallel in two independent experiments.

Statistical tests—All of statistics was analyzed using Prism 5.0. When only two groups were compared, two tailed unpaired Student's t-test was used. One-way ANOVA test was utilized to evaluate variation among more than two groups of datasets. The post hoc tests used include Dunnett's test for multiple comparisons obtained at the same experimental condition, and Bonferroni's test when the multiple comparisons were made from data produced at different conditions. All error bars indicate S.E.M. Detailed information of each statistical analysis is described in the figure legends.

Supplementary Material

Refer to Web version on PubMed Central for supplementary material.

Acknowledgments

We are grateful to Yishi Jin for reagents, the *Caenorhabditis* Genetics Center (NIH Office of Research Infrastructure Programs, P40 OD010440) and the National BioResource Project (Japan) for strains, and Seung-Jae V. Lee, Sunkyung Lee, members of the S.V. Lee and K. Kim Lab for helpful discussion and/or critical comments on the manuscript. We also thank members of the Advanced Neural Imaging Center in KBRI for their technical support. This work was supported by the DGIST R&D Program of the Ministry of Science, ICT and Future Planning (17-BD-06), KBRI Basic Research Program of the Ministry of Science, ICT and Future Planning (17-BR-04), and the National Research Foundation of Korea (NRF-2015R1D1A1A09061430, NRF-2017R1A4A1015534) (K.K.), NIH R15GM111094 (S.E.H), NIH R01GM087533 (R.A.B), KBSI Grant T37416 (Y.H.H), and KBRI Basic Research Program of the Ministry of Science, ICT and Future Planning (17-BR-02), and the Korea Health Technology R&D Project of the Ministry for Health and Welfare (HI14C1135) (K.J.L).

References

1. Beach FA, Jaynes J. Effects of early experience upon the behavior of animals. *Psychol Bull.* 1954; 51:239–263. [PubMed: 13167237]
2. Hensch TK. Critical period regulation. *Annu Rev Neurosci.* 2004; 27:549–579. [PubMed: 15217343]
3. Jeong PY, Jung M, Yim YH, Kim H, Park M, Hong E, Lee W, Kim YH, Kim K, Paik YK. Chemical structure and biological activity of the *Caenorhabditis elegans* dauer-inducing pheromone. *Nature.* 2005; 433:541–545. [PubMed: 15690045]
4. Butcher RA, Fujita M, Schroeder FC, Clardy J. Small-molecule pheromones that control dauer development in *Caenorhabditis elegans*. *Nat Chem Biol.* 2007; 3:420–422. [PubMed: 17558398]
5. Macosko EZ, Pokala N, Feinberg EH, Chalasani SH, Butcher RA, Clardy J, Bargmann CI. A hub-and-spoke circuit drives pheromone attraction and social behaviour in *C. elegans*. *Nature.* 2009; 458:1171–1175. [PubMed: 19349961]
6. Edison AS. *Caenorhabditis elegans* pheromones regulate multiple complex behaviors. *Curr Opin Neurobiol.* 2009; 19:378–388. [PubMed: 19665885]
7. Jang H, Kim K, Neal SJ, Macosko E, Kim D, Butcher RA, Zeiger DM, Bargmann CI, Sengupta P. Neuromodulatory state and sex specify alternative behaviors through antagonistic synaptic pathways in *C. elegans*. *Neuron.* 2012; 75:585–592. [PubMed: 22920251]
8. Lorenz K. Der Kumpan in der Umwelt des Vogels. *Journal für Ornithologie.* 1935; 83:137–213.
9. Hilliard MA, Bargmann CI, Bazzicalupo P. *C. elegans* responds to chemical repellents by integrating sensory inputs from the head and the tail. *Curr Biol.* 2002; 12:730–734. [PubMed: 12007416]
10. Srinivasan J, Kaplan F, Ajredini R, Zachariah C, Alborn HT, Teal PE, Malik RU, Edison AS, Sternberg PW, Schroeder FC. A blend of small molecules regulates both mating and development in *Caenorhabditis elegans*. *Nature.* 2008; 454:1115–1118. [PubMed: 18650807]
11. Sims JR, Ow MC, Nishiguchi MA, Kim K, Sengupta P, Hall SE. Developmental programming modulates olfactory behavior in *C. elegans* via endogenous RNAi pathways. *Elife.* 2016; 5
12. Hall SE, Beverly M, Russ C, Nusbaum C, Sengupta P. A cellular memory of developmental history generates phenotypic diversity in *C. elegans*. *Curr Biol.* 2010; 20:149–155. [PubMed: 20079644]
13. Hall SE, Chirn GW, Lau NC, Sengupta P. RNAi pathways contribute to developmental history-dependent phenotypic plasticity in *C. elegans*. *RNA.* 2013; 19:306–319. [PubMed: 23329696]
14. L'Etoile ND, Coburn CM, Eastham J, Kistler A, Gallegos G, Bargmann CI. The cyclic GMP-dependent protein kinase EGL-4 regulates olfactory adaptation in *C. elegans*. *Neuron.* 2002; 36:1079–1089. [PubMed: 12495623]
15. Remy JJ, Hobert O. An interneuronal chemoreceptor required for olfactory imprinting in *C. elegans*. *Science.* 2005; 309:787–790. [PubMed: 16051801]
16. Ikeda DD, Duan Y, Matsuki M, Kunitomo H, Hutter H, Hedgecock EM, Iino Y. CASY-1, an ortholog of calyntenins/alcadeins, is essential for learning in *Caenorhabditis elegans*. *Proc Natl Acad Sci U S A.* 2008; 105:5260–5265. [PubMed: 18381821]
17. Jin X, Pokala N, Bargmann CI. Distinct Circuits for the Formation and Retrieval of an Imprinted Olfactory Memory. *Cell.* 2016; 164:632–643. [PubMed: 26871629]
18. Bargmann CI, Hartweg E, Horvitz HR. Odorant-selective genes and neurons mediate olfaction in *C. elegans*. *Cell.* 1993; 74:515–527. [PubMed: 8348618]
19. Chou JH, Bargmann CI, Sengupta P. The *Caenorhabditis elegans* odr-2 gene encodes a novel Ly-6-related protein required for olfaction. *Genetics.* 2001; 157:211–224. [PubMed: 11139503]
20. Kim J, Yeon J, Choi SK, Huh YH, Fang Z, Park SJ, Kim MO, Ryoo ZY, Kang K, Kweon HS, et al. The Evolutionarily Conserved LIM Homeodomain Protein LIM-4/LHX6 Specifies the Terminal Identity of a Cholinergic and Peptidergic *C. elegans* Sensory/Inter/Motor Neuron-Type. *PLoS Genet.* 2015; 11:e1005480. [PubMed: 26305787]
21. White JG, Southgate E, Thomson JN, Brenner S. The structure of the nervous system of the nematode *Caenorhabditis elegans*. *Philos Trans R Soc Lond B Biol Sci.* 1986; 314:1–340. [PubMed: 22462104]

22. Gray JM, Hill JJ, Bargmann CI. A circuit for navigation in *Caenorhabditis elegans*. *Proc Natl Acad Sci U S A*. 2005; 102:3184–3191. [PubMed: 15689400]
23. Sagasti A, Hobert O, Troemel ER, Ruvkun G, Bargmann CI. Alternative olfactory neuron fates are specified by the LIM homeobox gene *lim-4*. *Genes Dev*. 1999; 13:1794–1806. [PubMed: 10421632]
24. Piggott BJ, Liu J, Feng Z, Wescott SA, Xu XZ. The neural circuits and synaptic mechanisms underlying motor initiation in *C. elegans*. *Cell*. 2011; 147:922–933. [PubMed: 22078887]
25. de Bono M, Maricq AV. Neuronal substrates of complex behaviors in *C. elegans*. *Annu Rev Neurosci*. 2005; 28:451–501. [PubMed: 16022603]
26. Giles AC, Rose JK, Rankin CH. Investigations of learning and memory in *Caenorhabditis elegans*. *Int Rev Neurobiol*. 2006; 69:37–71. [PubMed: 16492461]
27. Ardiel EL, Rankin CH. An elegant mind: learning and memory in *Caenorhabditis elegans*. *Learn Mem*. 2010; 17:191–201. [PubMed: 20335372]
28. Nevitt GA, Dittman AH, Quinn TP, Moody WJ Jr. Evidence for a peripheral olfactory memory in imprinted salmon. *Proc Natl Acad Sci U S A*. 1994; 91:4288–4292. [PubMed: 7514302]
29. Wilson DA, Sullivan RM. Neurobiology of associative learning in the neonate: early olfactory learning. *Behav Neural Biol*. 1994; 61:1–18. [PubMed: 7907468]
30. Golden JW, Riddle DL. A pheromone influences larval development in the nematode *Caenorhabditis elegans*. *Science*. 1982; 218:578–580. [PubMed: 6896933]
31. Izrayelit Y, Robinette SL, Bose N, von Reuss SH, Schroeder FC. 2D NMR-based metabolomics uncovers interactions between conserved biochemical pathways in the model organism *Caenorhabditis elegans*. *ACS Chem Biol*. 2013; 8:314–319. [PubMed: 23163760]
32. Guo ZV, Hart AC, Ramanathan S. Optical interrogation of neural circuits in *Caenorhabditis elegans*. *Nat Methods*. 2009; 6:891–896. [PubMed: 19898486]
33. Fujihara Y, Ikawa M. GPI-AP release in cellular, developmental, and reproductive biology. *J Lipid Res*. 2016; 57:538–545. [PubMed: 26593072]
34. Miwa JM, Ibanez-Tallon I, Crabtree GW, Sanchez R, Sali A, Role LW, Heintz N. *lynx1*, an endogenous toxin-like modulator of nicotinic acetylcholine receptors in the mammalian CNS. *Neuron*. 1999; 23:105–114. [PubMed: 10402197]
35. Tekinay AB, Nong Y, Miwa JM, Lieberam I, Ibanez-Tallon I, Greengard P, Heintz N. A role for *LYNX2* in anxiety-related behavior. *Proc Natl Acad Sci U S A*. 2009; 106:4477–4482. [PubMed: 19246390]
36. Gottschalk A, Schafer WR. Visualization of integral and peripheral cell surface proteins in live *Caenorhabditis elegans*. *J Neurosci Methods*. 2006; 154:68–79. [PubMed: 16466809]
37. Brenner S. The genetics of *Caenorhabditis elegans*. *Genetics*. 1974; 77:71–94. [PubMed: 4366476]
38. Coates JC, de Bono M. Antagonistic pathways in neurons exposed to body fluid regulate social feeding in *Caenorhabditis elegans*. *Nature*. 2002; 419:925–929. [PubMed: 12410311]
39. Tian L, Hires SA, Mao T, Huber D, Chiappe ME, Chalasani SH, Petreanu L, Akerboom J, McKinney SA, Schreier ER, et al. Imaging neural activity in worms, flies and mice with improved GCaMP calcium indicators. *Nat Methods*. 2009; 6:875–881. [PubMed: 19898485]
40. Kim K, Sato K, Shibuya M, Zeiger DM, Butcher RA, Ragains JR, Clardy J, Touhara K, Sengupta P. Two chemoreceptors mediate developmental effects of dauer pheromone in *C. elegans*. *Science*. 2009; 326:994–998. [PubMed: 19797623]
41. Srinivasan J, Durak O, Sternberg PW. Evolution of a polymodal sensory response network. *BMC Biol*. 2008; 6:52. [PubMed: 19077305]
42. Ibsen S, Tong A, Schutt C, Esener S, Chalasani SH. Sonogenetics is a non-invasive approach to activating neurons in *Caenorhabditis elegans*. *Nat Commun*. 2015; 6:8264. [PubMed: 26372413]
43. Chronis N, Zimmer M, Bargmann CI. Microfluidics for in vivo imaging of neuronal and behavioral activity in *Caenorhabditis elegans*. *Nat Methods*. 2007; 4:727–731. [PubMed: 17704783]
44. Kratsios P, Stolfi A, Levine M, Hobert O. Coordinated regulation of cholinergic motor neuron traits through a conserved terminal selector gene. *Nat Neurosci*. 2011; 15:205–214. [PubMed: 22119902]

HIGHLIGHTS

- Early pheromone exposure modulates behavioral responses to the pheromone as adults.
- Pheromone experience is imprinted as increased synaptic activity.
- The *odr-2* GPI-linked signaling protein mediates pheromone imprinting.

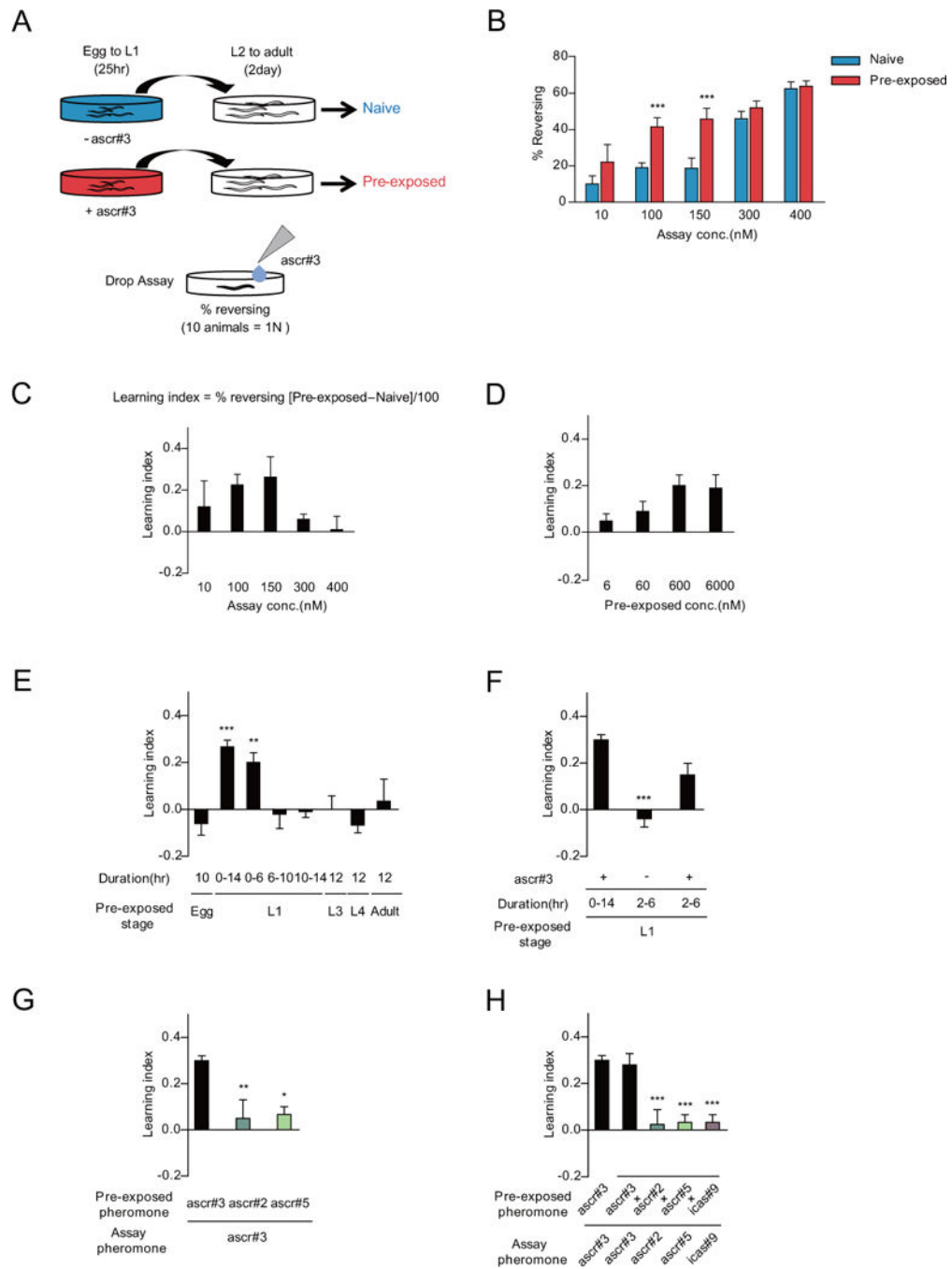


Figure 1. Transient exposure to the ascr#3 pheromone after birth specifically enhances ascr#3 avoidance behavior of adults

A. Experimental scheme of pheromone imprinting assay. The animals are exposed to dH₂O (naive: shown in blue) and ascr#3 diluted with dH₂O (pre-exposed: shown in red) from egg to the L1 stage. The percentage of reversal is calculated by measuring avoidance frequencies to ascr#3 exposure at the adult stage.

B and C. Percentage of reversal (B) and learning index (C) of naive and pre-exposed adult animals to 10 nM, 100 nM, 150 nM, 300 nM, and 400 nM ascr#3. Learning index is

calculated by the percentage of the reversal rate of pre-exposed minus the reversal rate of naive divided by 100. *** indicates different ascr#3 avoidance from naive at $p < 0.001$ by one-way ANOVA with Bonferroni's post hoc test. $n = 50-200$ each.

D. Learning index of adult animals pre-exposed to 6 nM, 60 nM, 600 nM and 6000 nM ascr#3 at L1. $n = 80-200$ each.

E. Learning index of adult animals pre-exposed to 600 nM ascr#3 at different developmental stages. Exposure times during the specific developmental stage are indicated as egg (10 hours), L3 (12 hours), L4 (12 hours) and adult (12 hours). For the L1 stage, exposure times are indicated as between starting and ending time of pheromone exposure. ** and *** indicate different from egg (10 hours) at $p < 0.01$ and $p < 0.001$ by one-way ANOVA with Dunnett's post hoc test, respectively. $n = 30-190$ each.

F. Learning index of adult animals exposed to ascr#3 for 4 hours in the L1 stage. Pre-exposure for 2-6 hour in the L1 stage is sufficient for ascr#3 imprinting. *** indicates different from ascr#3 pre-exposure for 14 hours at $p < 0.001$ by one-way ANOVA with Dunnett's post hoc test. $n = 80-120$ each.

G and H. Learning index of adult animals pre-exposed and/or assayed with other pheromone components. Animals are pre-exposed to either 600 nM ascr#3, ascr#2 or ascr#5 and assayed with 100 nM ascr#3 (G) and pre-exposed to pheromone mixture containing 600 nM ascr#3, ascr#2, ascr#5 and icas#9, and assayed with 100 nM ascr#3, ascr#2, ascr#5 or icas#9 (H). *, ** and *** indicate different from the control (ascr#3 pre-exposed and ascr#3 assayed) at $p < 0.05$, $p < 0.01$ and $p < 0.001$, respectively, by one-way ANOVA with Dunnett's post hoc test. (G) $n = 30-100$ each. (H) $n = 30-50$ each. (B-H) Error bars represent SEM. See also Figure S1.

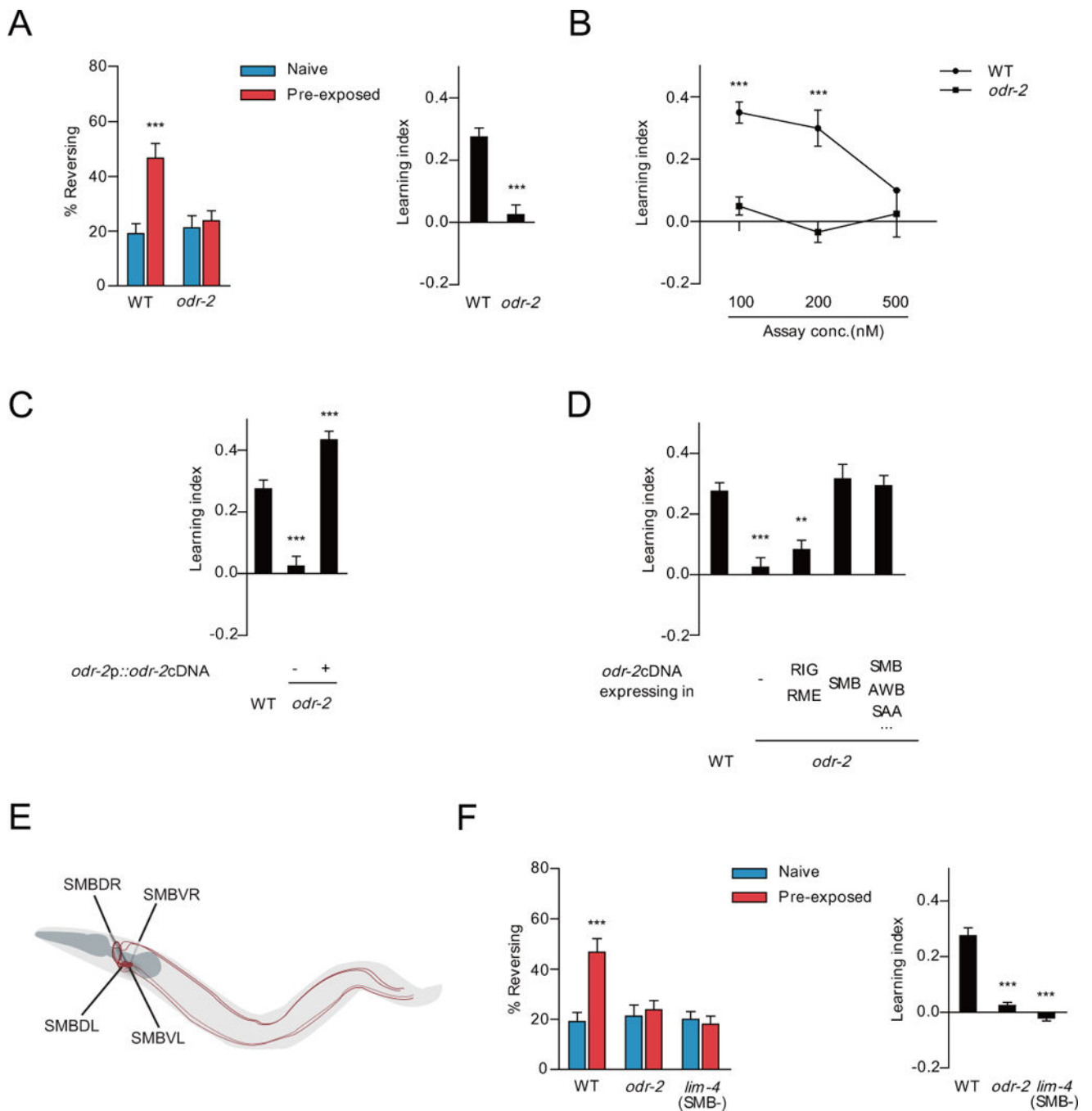


Figure 2. The glycosylated phosphatidylinositol-linked protein, ODR-2, is required for increased *ascr#3* avoidance in *ascr#3* imprinted animals

A. Percentage of reversal (left) and learning index (right) in wild-type and *odr-2* mutants. *** indicates significantly different from naive (left) and WT (right) at $p < 0.001$ by one-way ANOVA with Bonferroni's post hoc test (left) and by Student's t-test (right), respectively. $n = 80-120$ each.

B. Learning index of wild-type and *odr-2* mutants at 100 nM, 200 nM or 500 nM ascr#3. *** indicates different from WT at $p < 0.001$ by one-way ANOVA with Bonferroni's post hoc test. $n = 30-60$ each.

C and D. Learning index of wild-type and *odr-2* mutants expressing *odr-2* cDNA under the control of *odr-2* promoter (RIG, RME and SMB) (C) or cell specific promoters including *odr-2* (-377) (RIG and RME), *flp-12* (-339) (SMB), and *lim-4* (AWB, SAA, RID, RIV, RMD and SMB) (D). ** and *** indicate different from WT at $p < 0.01$ and $p < 0.001$, respectively, by one-way ANOVA with Dunnett's post hoc test. (C) $n = 80-120$ each. (D) $n = 60-140$ each.

E. Schematic diagram of the SMB neurons. A pair of dorsal and ventral cell bodies (SMBDs and SMBVs) are located in the head and their processes innervate head muscle and run posteriorly.

F. Percentage of reversal of naive and pre-exposed animals (left) and learning index (right) in wild-type, *odr-2*, and *lim-4* mutants. *** indicates different from naive (left) and WT (right) at $p < 0.001$ by one-way ANOVA with Bonferroni's (left) and Dunnett's post hoc tests (right), respectively. $n = 80-120$ each. All error bars represent SEM. See also Figure S2.

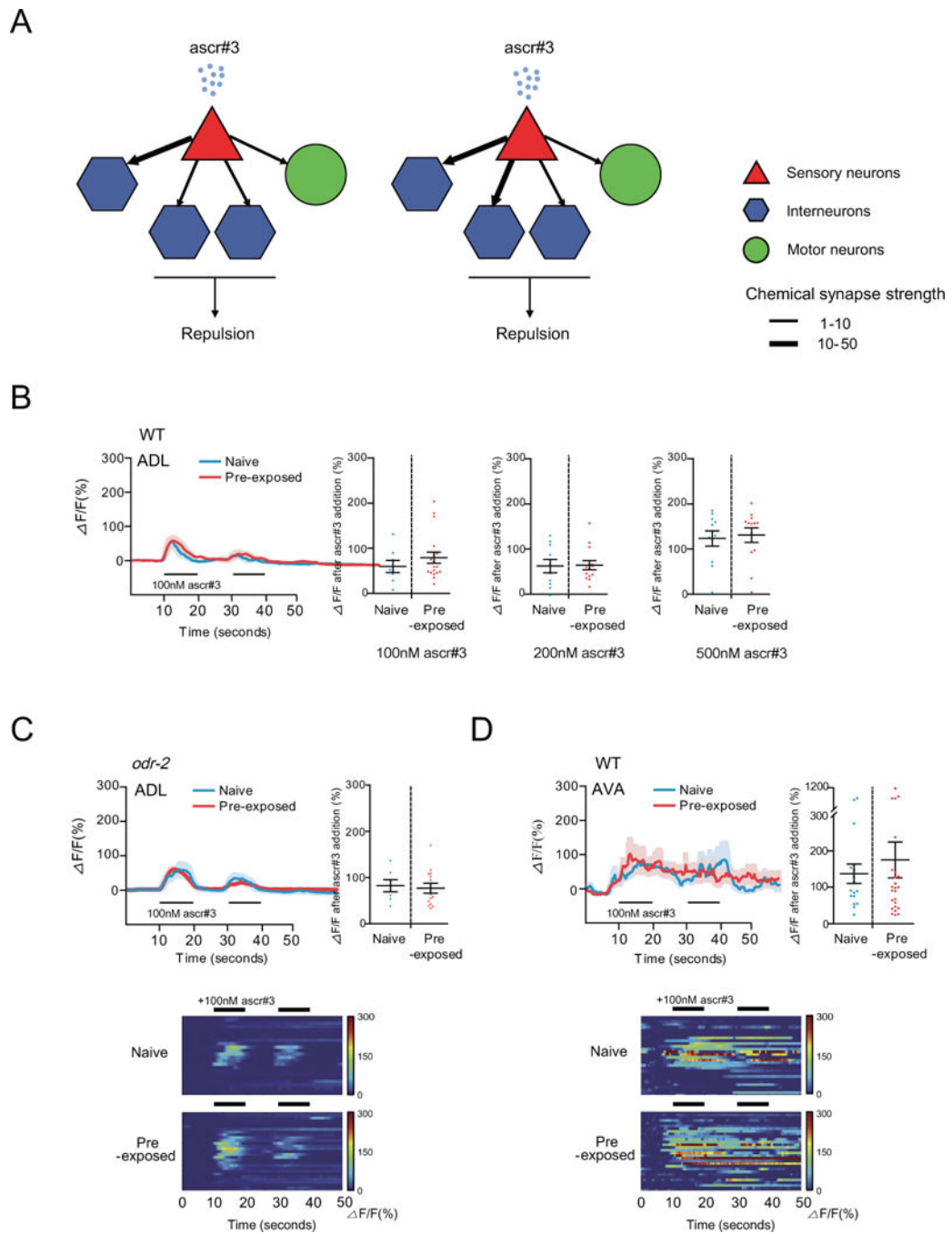


Figure 3. Ca^{2+} response to acute ascr#3 exposure is not altered in the ascr#3-sensing ADL neurons and their downstream command interneurons of ascr#3 imprinted animals

A. Post-synaptic connections of the ADLL and ADLR neurons. The AIB, AVD, AVA and SMBV neurons are post-synaptic to ADL. Chemical synapses between sensory (triangles), inter-(hexagons) and motor (circles) are indicated as arrows. Synaptic strength is indicated in thickness of lines (www.wormwiring.org).

B. Ca^{2+} transients of ADL in response to 100 nM ascr#3 exposure. The average traces of Ca^{2+} responses during two pulses of 100 nM ascr#3 (left) and the maximum value of Ca^{2+}

responses to 100 nM, 200 nM or 500 nM *ascr#3* (right) of naive (shown in blue) or pre-exposed animals (shown in red) in 50 seconds are shown. n=8 (naive) and 18 (pre-exposed) each.

C. Ca^{2+} transients of ADL in response to 100 nM *ascr#3* exposure in *odr-2* mutants. The average traces of Ca^{2+} responses during two pulses of 100 nM *ascr#3* (left), heat map of individual Ca^{2+} responses to *ascr#3* (bottom), and the maximum value of Ca^{2+} responses to 100 nM *ascr#3* (right) in naive (shown in blue) or pre-exposed (shown red) *odr-2* mutants are shown. n=7 (naive) and 14 (pre-exposed) each.

D. Ca^{2+} transients of AVA in response to 100 nM *ascr#3* exposure. The average traces of Ca^{2+} responses during two pulses of 100 nM *ascr#3* (left), heat map of individual Ca^{2+} responses to *ascr#3* (bottom), and the maximum value of Ca^{2+} responses to 100 nM *ascr#3* (right) in naive (shown in blue) or pre-exposed animals (shown in red) are shown. n=7 (naive) and 8 (pre-exposed) each. All error bars represent SEM.

See also Figure S3.

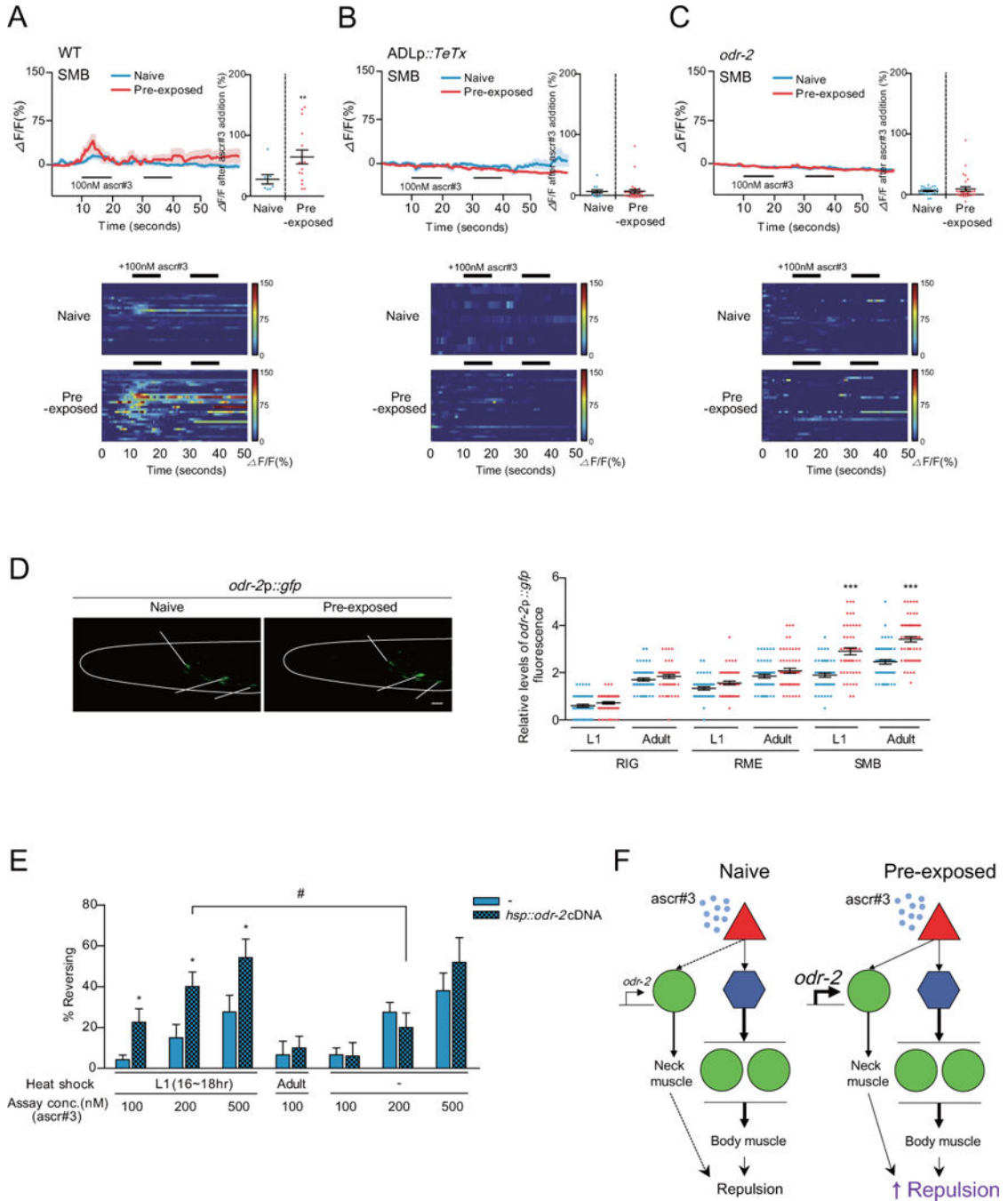


Figure 4. The SMB motor neurons mediate enhanced *ascr#3* avoidance in *ascr#3* imprinted animals

A–C. Ca^{2+} transients of the SMB neurons in response to 100 nM *ascr#3* in wild-type animals (A), wild-type animals expressing *ADLp::TeTx* (B) or *odr-2* mutants (C). The average traces of Ca^{2+} responses during two pulses of 100 nM *ascr#3* (left), heat map of individual Ca^{2+} responses to *ascr#3* (bottom), and the maximum value of Ca^{2+} responses to 100 nM *ascr#3* (right) in naive (blue) or pre-exposed animals [10] are shown. ** indicates different from naive at $p < 0.01$ by Student’s t-test. $n = 8–30$ each.

D. Representative images (left) and GFP quantification (right) of *odr-2p::gfp* expression in RIG, RME, and SMB of naive (shown in blue) and pre-exposed (shown in red) animals at the L1 or adult stages are shown. The images were taken of adults. *** indicates different from WT at $p < 0.001$ by one-way ANOVA with Bonferroni's post hoc test. $n = 50-60$ each. Scale bar: 10 μ m.

E. Percentage of reversal of adult transgenic animals expressing *hsp::odr-2* cDNA under heat shock at the L1 and adult stages. * indicates different from *hsp::odr-2* cDNA (-) and # indicates different from no heat shock at $p < 0.05$ by Student's t-test. $n = 50-70$ each. (A-E) Error bars represent SEM.

F. Model for circuit mechanisms underlying *ascr#3* avoidance in naive or *ascr#3* imprinted animals. In naive animals, ADL detects *ascr#3* and transmits the signals to the post-synaptic AVA command interneurons and downstream VA/DA motor neurons. In pre-exposed animals, the increased expression of *odr-2* in SMB initiates synaptic transmission from ADL to SMB that mediate *ascr#3* signal transmission from ADL not only to AVA but SMB. SMB activation may serve to sensitize background for backward movement via excitation of head muscles.

See also Figure S4.